Growth of Interdendritic Eutectic in Directionally Solidified Al-Si Alloys

R. GRUGEL and W. KURZ

Interdendritic eutectic microstructures in Al-Si (6 to 12.6 wt pct Si) alloys have been investigated as a function of growth velocity and temperature gradient. The interface morphology, as well as the behavior of the eutectic spacing and undercooling, suggest that the resultant microstructure is governed by two different growth processes. That is, at low growth rates, steady-state columnar eutectic growth is found and obeys the relationship, $\lambda^2 V$ = constant, where λ is the eutectic spacing and V is the growth rate. At higher growth rates, the nucleation of equiaxed eutectic grains occurs in the interdendritic liquid. The experimental findings are interpreted in the light of recently developed models for the columnar to equiaxed transition and for irregular eutectic growth.

I. INTRODUCTION

EUTECTIC and hypoeutectic Al-Si alloys are the basis of the most important group of light metal casting alloys.[1,2] Previous studies of these materials have focused on pure eutectic growth,[3-11] eutectic modification,[12-18] and the form of the coupled zone.[4,10,16,19-21] However, the growth of hypoeutectic alloys is not well understood, particularly with regard to the solidification behavior of the interdendritic eutectic. The latter is not only responsible for the good castability, but its volume fraction, morphology, and distribution have been shown to influence markedly the mechanical properties of these alloys.[22,23]

Toloui and Hellawell[8] found that, in alloys of eutectic composition, the eutectic flake spacings (λ) and interface undercoolings (ΔT) obeyed $\lambda \alpha V^{-1/2}$ and $\Delta T \alpha V^{1/2}$ relationships, respectively, as predicted by "regular" eutectic growth theory.[24] Here, V is the growth rate. However, both λ and ΔT were considerably greater than in the case of regular eutectics and, for a given growth rate, the spacing was reported to increase as the temperature gradient, G, in the liquid decreased.[8]

Elliott and Glenister[9] reexamined the silicon flake eutectic and found the spacing *vs* growth rate relationship to be of the form: $\lambda \alpha V^{-1/3}$. Their measured undercoolings were smaller than those previously reported[8] and they suggested two relationships: $\Delta T \alpha V^{1/4}$ at low growth rates, and $\Delta T \alpha V^{1/2}$ at higher rates. Furthermore, their work suggested that the temperature gradient did not significantly influence the undercooling at a given growth rate.

In this paper, the Al-Si eutectic will be further examined. However, the main aim is to investigate "irregular" interdendritic eutectic growth. The results will then be used to substantiate the previously reported[8,9] growth relationships in the light of Hunt's recent model for the columnar to equiaxed transition of eutectic and dendritic grains.[25]

II. EXPERIMENTAL PROCEDURE

In this study, aluminum-silicon alloys ranging in composition from 6 to 12.6 wt pct Si were examined. Aluminum (99.99 pct, major impurity 0.003 pct Fe) was first melted in a graphite crucible and the silicon (99.999 pct) was then added. After dissolution of the silicon, the well-stirred liquid was sucked up into 6 mm I.D. quartz tubes. The alloy rods were then machined to fit the 5 mm I.D. recrystallized alumina tubes used in the directional solidification experiments.

Two fine (0.1 mm) Pt-Pt 10 pct Rh thermocouples, protected by 0.5 mm O.D.-alumina sheaths, were used to determine the temperature. The leads near the bead were arranged parallel to the isotherms and the two thermocouples were spaced 5 mm apart along the growth direction. This arrangement was inserted directly into the molten alloy and, using a data acquisition system, the outputs from successive experimental runs were stored for later analysis.

The alloys were lowered vertically downward through a Bridgman type furnace at rates of between 1 and 300 $\mu m\ s^{-1}$. By noting the changes in slope of the recorded cooling curves as the solid-liquid interface passed the two thermocouples, the true growth rate of the interface could be determined. Spacing measurements were made in the central region of the specimen where the crucible velocity corresponded to the interfacial growth rate.

Initially, each specimen (5 mm in diameter, ~200 mm in length) was positioned in the furnace, with the solid-liquid interface at about 70 mm from the lower end. After a holding period, to allow temperature homogenization, the sample was lowered at a predetermined rate through about 70 mm. Growth was then interrupted by dropping the sample tube into a water spray.

Sample preparation consisted of a standard series of wet grinding and polishing steps, followed by etching in a solution of 60 ml H_2O, 10 g NaOH, and 5 g $K_3Fe(CN)_6$ for ~10 seconds.

Two different temperature gradients (5 and 15 Kmm^{-1}) were employed. These were determined from the linear portion of the temperature trace recorded in the liquid just ahead of the dendrite tips (hypoeutectic alloys) or ahead of the solid-liquid interface (eutectic alloys). The positions of these interfaces and their undercoolings, as detected by the change in slope of the cooling curve, were further verified by metallographic examination of several samples with quenched-in thermocouples.

It was found that the measured temperature gradient varied along the length of the dendrites. At all growth rates it was observed that, for alloys with 6, 10, and 12 wt pct Si and for a temperature gradient of 15 Kmm^{-1} in the liquid at

R. GRUGEL, Postdoctoral Associate, and W. KURZ, Professor, Department of Materials, are with the Swiss Federal Institute of Technology, CH-1007 Lausanne, Switzerland.

Manuscript submitted May 8, 1986.

the initial solid-liquid interface, the gradients at the eutectic interface were 9, 12.5, and 15 Kmm^{-1}, respectively. This was a result of the change in volume fraction of the primary dendrites with composition. The gradients referred to below will be those in the liquid at the first solid to form, *i.e.*, 5 and 15 Kmm^{-1}.

Within the ranges of growth rate and temperature gradient used, a eutectic structure consisting of flake silicon in an aluminum matrix was always observed. The flake spacing in the eutectic was measured by using the procedure described by Toloui and Hellawell.[8] Lines were drawn at right angles to parallel flakes on sections cut perpendicularly to the growth direction, the spacing being determined by the number of intercepts. No geometrical correction for the 3rd dimension was included in this analysis since it only slightly modifies the results, as seen from their Table I. At least 15 representative measurements of the eutectic spacing were made on each sample. The data points represent the mean of the measurements which had, in general, an average deviation of ±8.5 pct.

Finally, it should be mentioned that the similar densities of the components served to minimize convection effects at the solid-liquid interface.

III. RESULTS

Figure 1 shows the spacing results, measured in the eutectic regions of all directionally solidified samples, as a function of growth rate and temperature gradient. Lines representing the experimental results of Toloui and Hellawell[8] and Elliott and Glenister[9] are included for comparison.

At growth rates below 25 $\mu m\ s^{-1}$, the spacing measurements for samples solidified under a temperature gradient of 5 Kmm^{-1} are similar to those for a gradient of 15 Kmm^{-1}. This suggests that the gradient does not have as great an effect upon the eutectic spacing as previously thought. A linear regression analysis of these data, according to $\lambda \alpha V^{-n}$, resulted in an exponent of $n = 0.41$. This is somewhat smaller than the theoretical value of 0.5 which is predicted for regular eutectic growth. At growth rates greater than 30 $\mu m\ s^{-1}$, the spacing was found to decrease less with increasing velocity, the values for the lower gradient being greater than those for the higher one. A regression analysis of the points for $V > 30\ \mu m\ s^{-1}$ gives a mean value of $n = 0.2$ for $G = 5\ Kmm^{-1}$, and 0.25 for $G = 15\ Kmm^{-1}$.

Table I. Phase Diagram Parameters and Material Constants Used in This Study[27]

T_E	577.2C
$\lvert m \rvert_{Al}$	7.5 K/wt pct
m_{Si}	17.5 K/wt pct
C_0	98.2 wt pct
D_L	$3 \times 10^{-9}\ m^2\ s^{-1}$
Γ_{Al}	9×10^{-8} mK
Γ_{Si}	2×10^{-7} mK
θ_{Al}	25 deg
θ_{Si}	85 deg
f_{Si}	0.127
P	8.9×10^{-3}

Figures 2(a) and (b) are representative of the interdendritic eutectic and the pure eutectic interface observed at growth rates below 30 $\mu m\ s^{-1}$. In general, the eutectic interface is macroscopically flat and growth is columnar. There is no obvious difference in the flake spacing, which suggests a minimal effect of the local gradients at the eutectic front (between 9 and 15 Kmm^{-1}) or of the presence of primary dendrites.

In the sample shown in Figure 3 grown at $V = 32.6\ \mu m\ s^{-1}$, no coherent eutectic interface exists and equiaxed eutectic grains can be observed. Nucleation is first discerned at point A and eutectic growth appears to be complete at B. This distance corresponds to 0.55 mm. With a local gradient of 4 Kmm^{-1} and a temperature interval of 2.2 K, a solidification time of ~17 seconds is available for the growth of these eutectic grains. For both of the temperature gradients employed in this study, an interface of this type was found

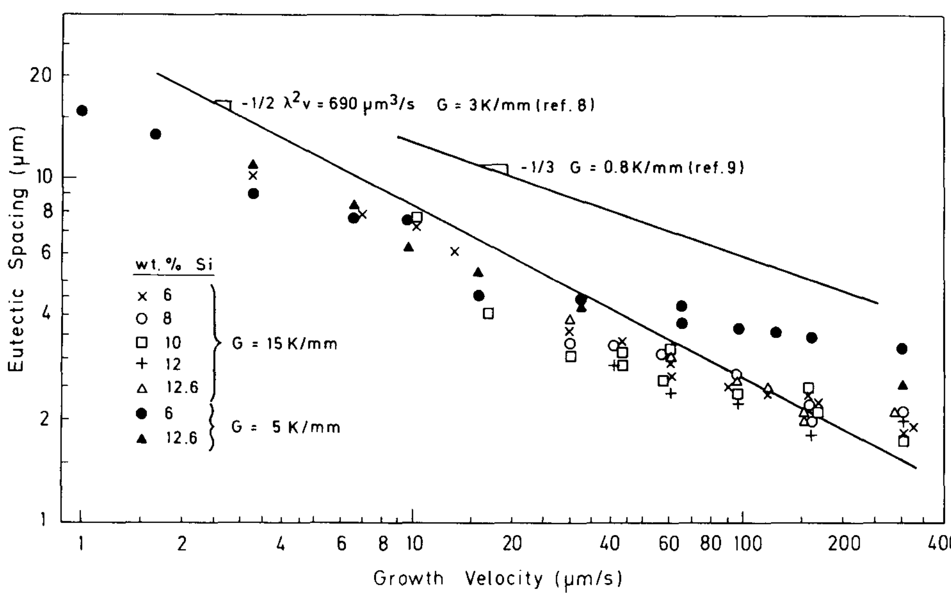

Fig. 1—Eutectic spacings for Al-Si alloys as a function of growth rate for two temperature gradients (5 and 15 Kmm^{-1}). Points from this study, lines from Toloui and Hellawell,[8] and Elliott and Glenister.[9]

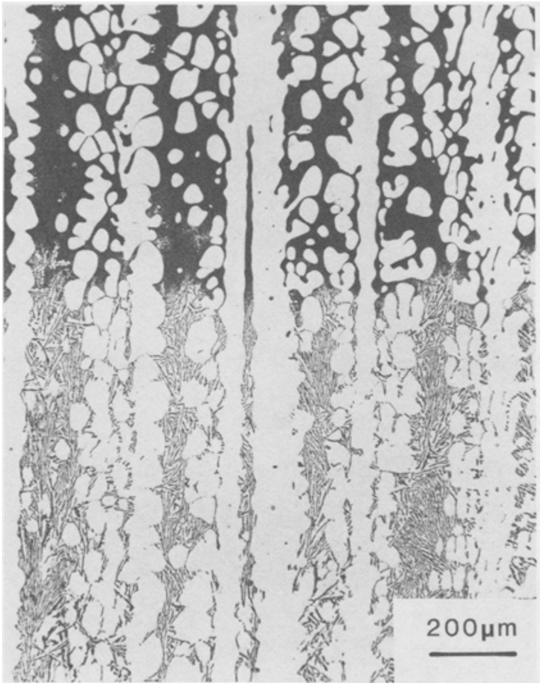

(a)

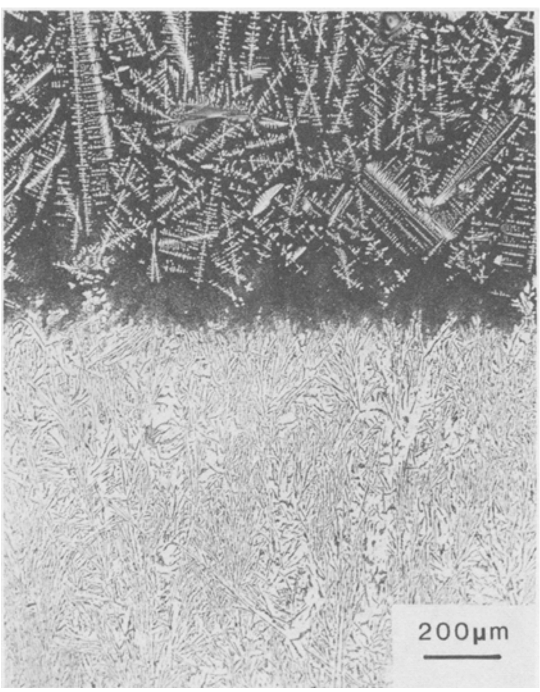

(b)

Fig. 2—Longitudinal section showing columnar growth of the eutectic at $V = 29\ \mu m\ s^{-1}$ and $G = 15\ Kmm^{-1}$: (a) interdendritic eutectic in Al-8 wt pct Si, (b) Al-12.6 wt pct Si. (White phase: Al, black phase: quenched liquid above and Si below eutectic interface.)

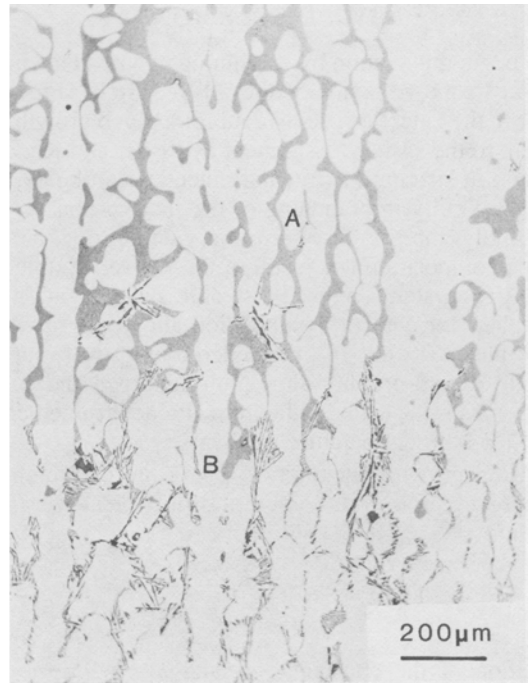

Fig. 3—Longitudinal section showing equiaxed growth of eutectic grains between dendrites in an Al-6 wt pct Si alloy at $V = 32.6\ \mu m\ s^{-1}$ and $G = 5\ Kmm^{-1}$. (A) start and (B) end of grain growth.

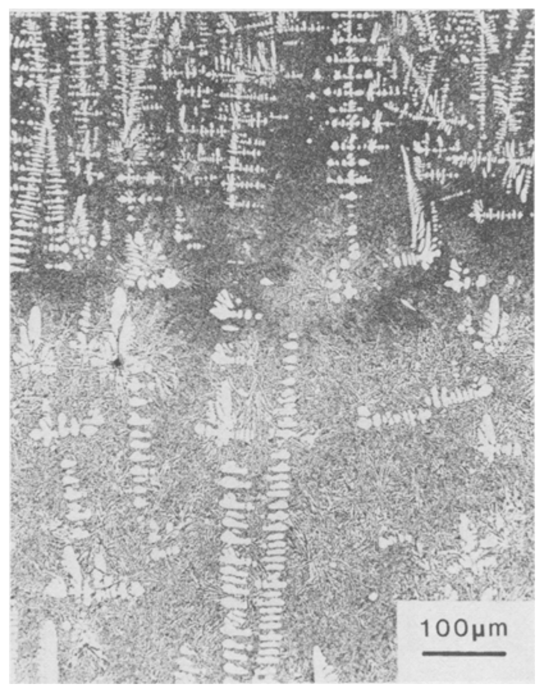

Fig. 4—Longitudinal section showing the equiaxed eutectic growth front of an Al-12.6 wt pct Si alloy at $V = 300\ \mu m\ s^{-1}$ and $G = 15\ Kmm^{-1}$.

for alloys grown at rates greater than $30\ \mu m\ s^{-1}$. Equiaxed eutectic grains become more prevalent at higher velocities and lower temperature gradients.

This effect is also observed in alloys of eutectic composition. Figure 4 shows a macroscopically irregular interface, ahead of which equiaxed eutectic grains are seen. There is no sign of aligned eutectic growth.

The results will now be discussed in the light of present theories, with particular regard to the spacings measured in alloys grown at rates above and below $30\ \mu m\ s^{-1}$.

IV. DISCUSSION

We begin this section by examining two results which are relevant to the behavior of the Al-Si system. Firstly, the scatter in the eutectic spacing data for a given growth rate is inherent to the system. As argued by Fisher and Kurz,[26] the variation in spacing of irregular eutectics can be explained by the difficulty in branching of the faceted phase.

Secondly, the presence of primary dendrites in alloys of eutectic composition is a result of the skewed coupled zone of the Al-Si system. In the course of this investigation it was found that, for eutectic composition alloys at growth rates greater than ~30 μm s^{-1}, the undercoolings were sufficient to produce both primary aluminum dendrites and eutectic. This is consistent with the theoretically determined coupled zone[21] for both temperature gradients.

Eutectic growth calculations, using the extremum condition (*e.g.*, minimum undercooling), lead to the relationships:[24]

$$\lambda_{ex}^2 V = K_2/K_1 \qquad [1]$$

$$\Delta T_{ex}^2/V = 4K_1K_2 \qquad [2]$$

Evaluation of the constants, K_1 and K_2, using the phase diagram parameters and material properties of the Al-Si system (Table I[27]), results in:

$$K_1 = 1.38 \times 10^{-2}\, K\, s\, \mu\text{m}^{-2} \qquad [3]$$

and

$$K_2 = 1\, K\, \mu\text{m}. \qquad [4]$$

The spacing *vs* growth rate relationship is then $\lambda_{ex}^2 V = 72.5\ \mu\text{m}^3\ \text{s}^{-1}$, and is plotted in Figure 5. A least squares fit to the experimental points representing the mean values of the lamellar spacings $\langle\lambda\rangle$ for $V < 25\ \mu\text{m s}^{-1}$, and the use of Eq. [1], gives $\langle\lambda\rangle^2 V = 382\ \mu\text{m}^3\ \text{s}^{-1}$. This indicates that $\langle\lambda\rangle$ is larger than λ_{ex}.

In faceted nonfaceted systems, an average spacing $\langle\lambda\rangle$ lying between the extremum, λ_{ex}, and branching, λ_{br}, values has been defined. Following the procedure suggested by Jones and Kurz,[28] the average spacing can be related to λ_{ex} and λ_{br} by:

$$\langle\lambda\rangle = \varphi\lambda_{ex} = \frac{\lambda_{ex} + \lambda_{br}}{2} \qquad [5]$$

From the results presented in Figure 5, it is found that $\varphi = 2.3$. the spacing *vs* growth rate relationship can then be given as:[28]

$$\langle\lambda\rangle^2 V = \varphi^2 \frac{K_2}{K_1} \qquad [6]$$

The branching spacing can be obtained from Eq. [5] as

$$\lambda_{br} = (2\varphi - 1)\lambda_{ex} \qquad [7]$$

leading to $\lambda_{br} = 3.6\ \lambda_{ex}$. The corresponding spacing is also shown in Figure 5.

Similarly, the average undercooling $\langle\Delta T\rangle$ as a function of growth velocity can be determined.[28]

$$\langle\Delta T\rangle = \frac{1}{\varphi}(1 + \varphi^2)\sqrt{K_1K_2V} = 1.37\ \Delta T \qquad [8]$$

Equation [8] is plotted in Figure 6, together with the experimentally measured eutectic undercoolings for several samples. Only data from samples grown at velocities less than 30 μm s^{-1} are included. Despite the inevitable scatter in such measurements, the experimental points agree with the predicted mean undercooling $\langle\Delta T\rangle$, thus confirming the consistency of the analysis.

In the treatment of the measured eutectic spacings at growth rates greater than 30 μm s^{-1}, steady state columnar growth cannot be assumed. Recently, Hunt[25] has discussed the transition from columnar to equiaxed growth occurring during eutectic and dendritic solidification and has developed a theoretical relationship which shows that equiaxed growth is preferred at low temperature gradients and high growth rates, and when nucleation sites are readily available.

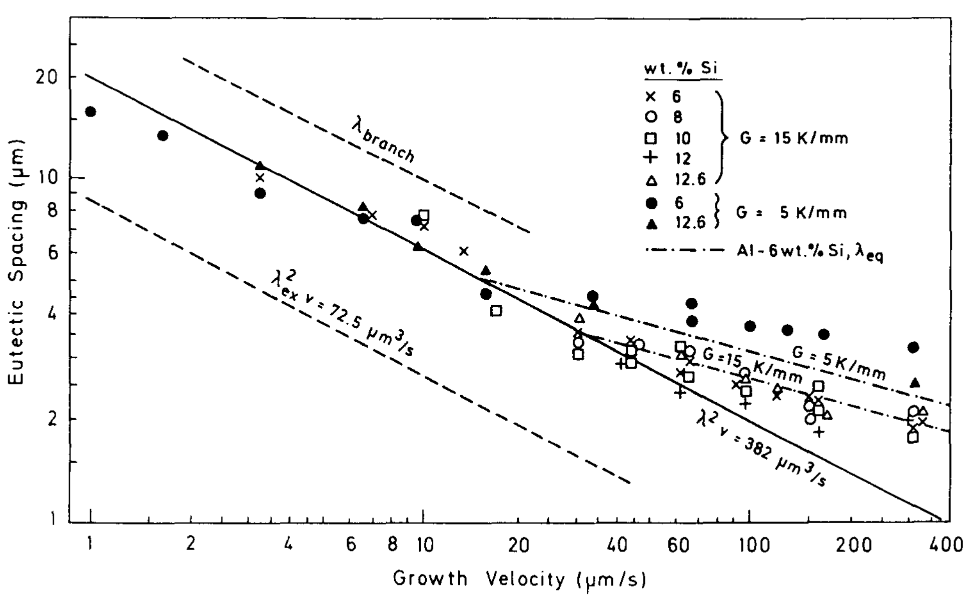

Fig. 5 — Comparison of the eutectic spacing measurements with the analysis of — Jones and Kurz,[28] —·—·— Hunt.[25]

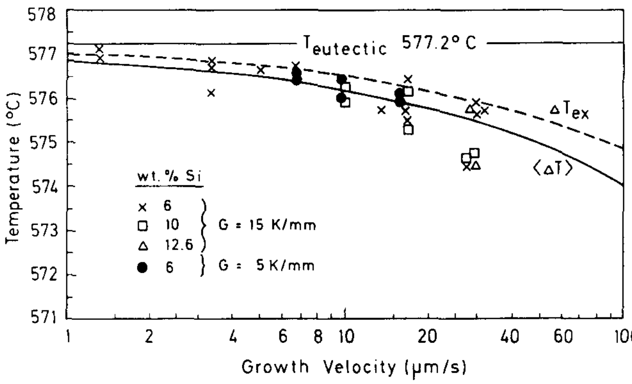

Fig. 6—Measured eutectic undercoolings as a function of growth rate. Lines correspond to theory: --- undercooling, ΔT_{ex}, according to the extremum criterion, — average undercooling, $\langle \Delta T \rangle$, for columnar eutectic growth.

We follow Hunt[25] for the case of negligible nucleation undercooling. For metals, the growth undercooling for equiaxed grains is assumed to be identical to that for columnar grains, given by Eq. [2]:

$$\Delta T = \left(\frac{V'}{A}\right)^{1/2} \qquad [9]$$

where A is a constant. The only difference between Eqs. [2] and [9] is in the definition of V. In the first case, V corresponds to the velocity of the solid-liquid interface in the direction of crucible movement (equal to the rate of crucible displacement under steady state conditions). In the second case (equiaxed growth), V' is the radial growth rate of the equiaxed grain, and might be very different from V.

The eutectic lamellar spacing for columnar or equiaxed growth is related to the growth undercooling by

$$\lambda = \frac{B}{\Delta T} \qquad [10]$$

where B is a constant. For fully equiaxed growth, one can evaluate the radius of a grain from:

$$r = \int_0^t V' \, dt \qquad [11]$$

Substituting V' from Eq. [9] into Eq. [11], noting that

$$-V \cdot G = \frac{dT}{dt} = -\frac{d(\Delta T)}{dt} \qquad [12]$$

i.e., $dt = d(\Delta T)/(VG)$, and integrating between $\Delta T = 0$ and ΔT gives:

$$r = \frac{A(\Delta T)^3}{3VG} \qquad [13]$$

Replacing Eq. [10] for ΔT in Eq. [13] gives

$$\lambda = B\left[\frac{A}{3VGr}\right]^{1/3} \qquad [14]$$

which relates the eutectic spacing to the grain radius. Expressing A and B in terms of K_1 and K_2 gives

$$A = \frac{V}{\Delta T^2} = \left(\frac{\varphi}{1 + \varphi^2}\right)^2 \frac{1}{K_1 K_2} \qquad [15]$$

and

$$B = \lambda \Delta T = (1 + \varphi^2) K_2 . \qquad [16]$$

The corresponding values for the alloy considered are $A = 9.7\ \mu\text{m}/K^2 s$ and $B = 6.3\ K\ \mu\text{m}$.

The radii of the interdendritic grains, r, are limited by the lateral extent of the interdendritic liquid. One can write:

$$r \simeq f_i \lambda_1 \qquad [17]$$

where f_i is a geometric factor. From the observation of metallographic sections one finds that, for 6 to 8 wt pct Si alloys, $f_i \sim 0.1$. (For example, in Figure 2(a), λ_1 is approximately 300 μm and the interdendritic eutectic has a lateral extent of $2r \simeq 50$ to 100 μm.)

The primary spacing, λ_1, of the dendrites can be shown to be[27]

$$\lambda_1 = \frac{4.3(\Delta T_0 D \Gamma)^{1/4}}{k^{1/4} V^{1/4} G^{1/2}} \qquad [18]$$

which leads, for Al-6 wt pct Si, to

$$r = 3.6 \cdot 10^{-4}\ V^{-1/4}\ G^{-1/2}\ [\text{m}] \qquad [19]$$

Eqs. [19] and [14] lead to the relationship for the spacing of the equiaxed interdendritic Al-Si eutectic:

$$\lambda = 1.31 \cdot 10^{-6}\ V^{-1/4}\ G^{-1/6}\ [\text{m}] \qquad [20]$$

Equation [20] is shown in Figure 5 for two gradients (5 and 15 K/mm). Comparison with the experimental points reveals a reasonable agreement. Theory, as well as the experimental results, indicate a $\lambda^4 V$-type relationship, and the critical velocity for the transition from columnar to equiaxed eutectic growth increases from 15 to 30 μm s^{-1} upon increasing the gradient from 5 to 15 Kmm^{-1}.

In view of the above, it is seen that steady state columnar growth of the irregular Al-Si eutectic occurs at low growth rates and high temperature gradients, and closely follows the $\lambda^2 V$ = constant relationship. At higher growth rates or lower temperature gradients, nucleation and growth of equiaxed eutectic grains occurs and results in an average eutectic spacing described by $\lambda^2 V'$ = const. (where V' is the growth rate of the equiaxed grains). The spacing of the equiaxed eutectic is greater than predicted by the $\lambda^2 V$ relationship determined from the region of columnar growth (where V is the crucible velocity).

Therefore, as Hunt has already pointed out, exponents smaller than ½ in the λ-V relationship, which have often been observed for irregular eutectics (Figure 1), can be explained by the occurrence of equiaxed growth. The reason for this change is therefore believed to be found not in eutectic growth behavior differing from $\lambda^2 V$ = const., but rather in the fact that, in equiaxed growth, the crucible displacement rate is quite different from the growth rate of the grains.

V. CONCLUSIONS

1. Eutectic spacing measurements in pure hypoeutectic and eutectic Al-Si alloys have been made as a function of growth rate and temperature gradient. At low rates, aligned steady state directional growth is observed which

obeys the well-known relationship, $\lambda^2 V$ = const. (where the const. is 382 μm^3 s^{-1}).

2. At higher rates, nucleation and growth of equiaxed eutectic grains in the interdendritic liquid is observed. In this range, the spacing obeys instead a $\lambda^4 V$ = const. relationship (where V is the crucible displacement rate). Such a λ-V relationship can be rationalized by assuming that growth of the equiaxed grains follows the same growth behavior as that of columnar grains and by considering the available interdendritic space, which depends upon the primary dendrite spacing.
3. At low growth rates, the columnar eutectic spacing seems to be independent of the temperature gradient. At higher rates, nucleation occurs ahead of the front and results in measured spacings which are greater than those expected for columnar growth. This spacing decreases with increasing temperature gradient. Furthermore, the transition velocity is found to increase with increasing temperature gradient. These results are in accordance with the theory presented by Hunt.
4. Under steady state (columnar) growth conditions, the eutectic spacing in alloys of eutectic composition is the same as in the interdendritic regions of off-eutectic alloys.
5. An analysis of the measured undercoolings further confirms the validity of the $\lambda^2 V$ = constant and $\Delta T^2/V$ = constant relationships for the faceted nonfaceted Al-Si eutectic under columnar and equiaxed growth conditions.

ACKNOWLEDGMENTS

The authors acknowledge helpful discussions with Dr. M. Rappaz and Dr. P. Magnin, and the collaboration of M. Gremaud. This research was conducted as part of the Swiss National Project on "Materials and Material Resources" which is supported by the Swiss National Foundation for Scientific Research.

REFERENCES

1. D. Mietrach and J. Weilke: *Aluminium*, 1982, vol. 58, p. 157.
2. R. Elliott: *Eutectic Solidification Processing*, Butterworths, 1983, London.
3. M. G. Day and A. Hellawell: *Proc. Roy. Soc. A*, 1968, vol. 305, p. 473.
4. H. A. H. Steen and A. Hellawell: *Acta Metall.*, 1972, vol. 20, p. 363.
5. L. Vandenbulcke and G. Vuillard: *J. Cryst. Growth*, 1972, vol. 12, pp. 137 and 145.
6. A. J. McLeod, L. M. Hogen, C. McL. Adam, and D. C. Jenkinson: *J. Cryst. Growth*, 1973, vol. 19, p. 301.
7. H. A. H. Steen and A. Hellawell: *Acta Metall.*, 1975, vol. 23, p. 529.
8. B. Toloui and A. Hellawell: *Acta Metall.*, 1976, vol. 24, p. 565.
9. R. Elliott and S. M. D. Glenister: *Acta Metall.*, 1980, vol. 28, p. 1489.
10. O. A. Atasoy, F. Yilmaz, and R. Elliott: *J. Cryst. Growth*, 1984, vol. 66, p. 137.
11. A. Gruber, F. Jeglitsch, and W. Köck: *Z. Metallkde.*, 1984, vol. 75, p. 341.
12. V. de L. Davies and J. M. West: *J. Inst. Metals*, 1963, vol. 92, p. 175.
13. M. G. Day and A. Hellawell: *J. Inst. Metals*, 1967, vol. 95, p. 37.
14. M. F. X. Gigliotti and G. A. Colligan: *Metall. Trans.*, 1972, vol. 3, p. 933.
15. H. Fredriksson, M. Hillert, and N. Lange: *J. Inst. Metals*, 1973, vol. 101, p. 285.
16. P. C. Jenkinson and L. M. Hogan: *J. Cryst. Growth*, 1975, vol. 28, p. 171.
17. S. M. D. Glenister and R. Elliott: *Metal Sci.*, 1981, p. 181.
18. N. Eustathopoulos and S. Bercovici: *Mém. Scient. Rev. Métall.*, 1984, p. 625.
19. E. Scheil: *Giesserei*, 1959, vol. 24, p. 1313.
20. G. A. Chadwick: in *The Solidification of Metals*, The Iron and Steel Institute, London, 1968, p. 138.
21. W. Kurz and D. J. Fisher: *Intern. Met. Rev.*, 1979, p. 177.
22. E. Blank and M. Rappaz: in *Comportement plastique des solides anisotropes*, J. P. Boehler, ed., Colloques intern. CNRS No 319, 1982, Edition du CNRS Paris, 1985, p. 257.
23. E. Blank, W. Kurz, and M. Rappaz: *Helvetica Phys. Acta*, 1985, vol. 58, p. 469.
24. K. A. Jackson and J. D. Hunt: *TMS-AIME*, 1966, vol. 236, p. 1129.
25. J. D. Hunt: *Mater. Sci. Eng.*, 1984, vol. 65, p. 75.
26. D. J. Fisher and W. Kurz: *Acta Metall.*, 1980, vol. 28, p. 777.
27. W. Kurz and D. J. Fisher: *Fundamentals of Solidification*, Trans. Tech. Publications, 4711 Aedermannsdorf, Switzerland, 1984.
28. H. Jones and W. Kurz: *Z. Metallkde.*, 1981, vol. 72, p. 792.